worldwide infected with HBV, more than 350 million remain chronically infected and become carriers of the virus [3]. Epidemiological studies have uncovered chronic HBV infection as the major etiological factor in the development of hepatocellular carcinoma (HCC) [4]. Despite the availability of an efficient vaccine, persistent HBV infection remains a challenging global health issue. The recent discovery of miRNAs involvement in HBV infection provides new insights into the virus biology and pathogenesis [5,6].

This chapter will outline the roles of miRNAs in the HBV biology and associated pathogenesis. We will also outline present and future miRNA-based strategies for the diagnosis, prognosis and treatment of the HBV-related diseases.

2. Biogenesis and Functions of miRNAs

miRNAs are most commonly transcribed in the nucleus by the RNA polymerase II (Pol II), as monocistronic or polycistronic pri-miRNAs that are further processed in pre-miRNAs (Figure 1). These pre-miRNAs are exported to the cytoplasm where they undergo cleavage by the RNAse III enzyme called Dicer that produces a miRNA duplex. This duplex splits to generate the single-stranded mature miRNA that incorporates the RNA-induced silencing complex (RISC). Based on the complementarity with its target gene sequence, the mature miRNA induce either translational repression (partial complementarity) or mRNA degradation (perfect complementarity) [7]. Besides, the mature miRNA can increase the expression of the target gene under growth arrest condition [8]. Finally, it has been recently reported that miRNA can also act in a RISC-independent manner on the transcriptional level by interaction with ribonucleoprotein or direct binding to DNA [9–11].

One single miRNA has the ability to regulate multiple targets and thereby to affect a broad network of genes (up to 100 genes) [12]. This specific characteristic makes the miRNAs key mediators of most of the cellular events. In animal, miRNAs mainly regulate mRNAs by interacting with their 5' end (5p) to the 3'-untranslated region (3'-UTR) of their target [13]. However, recent studies have revealed miRNAs target sites in the 5'-UTR, which interacts with the 3' end (3p) of miRNAs, and even simultaneous 5'-UTR and 3'-UTR interaction sites [14,15].

The abnormal expression levels of miRNAs have been revealed in various diseases such as cancer [16,17], inflammation [18,19], Alzheimer [20], cardiovascular disease [21] and viral infection including HBV [2,22].

3. Role of miRNAs in HBV Infection

Despite the fact that HBV is a nuclear DNA virus, none viral-encoded miRNA has been so far identified. Only one putative HBV miRNA, with hypothetical regulation role on its own genome, was deduced by computational approach [23]. However, HBV can modulate the expression of several cellular miRNAs in order to promote a favorable environment for its replication and survival. They are presented in this section and summarized in Table 1.

3.1. Brief Description of HBV Infection

The HBV infection is characterized by two phases; the acute and the chronic infection [24]. The initial stages of the acute infection include virion attachment [25], uncoating and nucleocapsid transport to the cell nucleus (Figure 2, steps 1 and 2). The 3.2 kb relaxed circular DNA genome is released into the nucleus and converted into a covalently closed circular DNA (cccDNA) from which all the viral RNAs are transcribed (Figure 2, steps 3 to 5). The pregenomic RNA (pgRNA) serves as template for reverse transcription (Figure 2, steps 8 and 9). The subgenomic mRNAs comprise the pre-surface (S) and S genes, the pre-core (C) and C genes, the polymerase gene, and the X gene. The newly formed nucleocapsids can either assemble with envelope proteins in the endoplasmic reticulum and form mature virions that will be secreted (Figure 2, steps 10 and 11), or return to the nucleus to maintain the cccDNA amplification. When the immune system fails to clear the virus, the HBV infection becomes chronic and it remains under a dormant state into the cell. Eventually, the viral genetic material or sequences can integrate into the host cellular DNA. The integration has been frequently observed and is associated with HCC [26,27].

Figure 1. Schematic representation of miRNA biogenesis. The mature miRNAs originate from successive different steps. An initial DNA transcription generates pri-miRNAs that are cleaved in pre-miRNAs before their exportation to the cytoplasm. There, an RNAse III enzyme, Dicer, cleaves it to generate a miRNA duplex that subsequently joins an RNA-induced silencing complex (RISC) to produce the mature miRNA. The sequence complementarity to the target will decide its fate. Some miRNAs can act on the transcriptional level independently from the RISC.

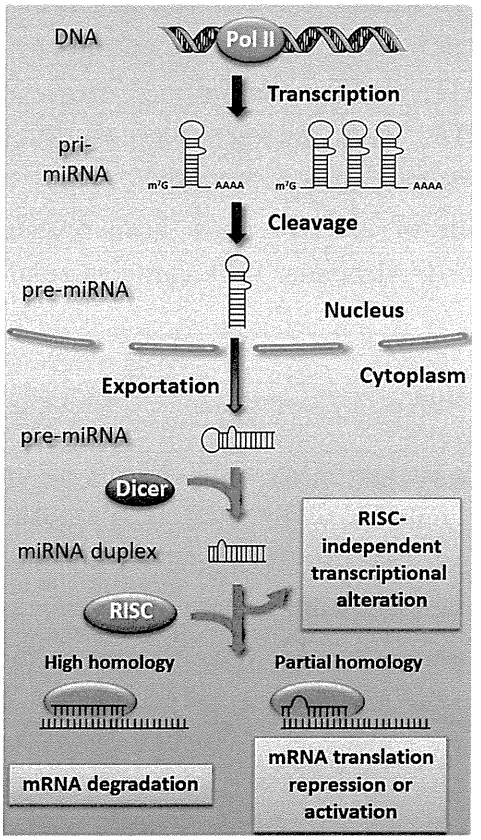

Table 1. Cellular miRNAs and their effects on HBV infection or HBV related-diseases. HBV (↑): Promotes HBV replication; HBV (↓): Inhibits HBV replication; HCC (↑): Development and/or growth of HCC; Fibrosis (↑): Promotes liver fibrosis.

miRNAs	miRNA expression	Target genes	HBV or disease status	Ref.
		Cellular targets		
miR-1	up	HDAC4 (histone deacetylase 4)	HBV (↑)	[28]
miR-17-92 cluster	up	E2F1 (c-myc repressor)	HBV (↑?), HCC (↑)	[29]
miR-155	up	C/EBPβ (CCAAT/enhancer binding protein)	HCC (↑)	[30]
		SOCS1 (JAK/STAT signaling)	HBV (↓)	[31]
miR-181a	up	HLA-A? (MHC class I)	HBV (↑)	[5]
miR-372	up	NFIB (nuclear factor I/B)	HBV (↑)	[32]
miR-373	up	NFIB (nuclear factor I/B)	HBV (↑)	[32]
miR-501	up	HBIP (HBx inhibitor)	HBV (↑)	[33]
mir-29 family	down	collagen	Fibrosis (↑)	[22,34]
miR-122	down	cyclin G1 (p53 modulator)	HBV (↑), HCC (↑)	[6]
miR-152	down	DNMT1 (DNA methyltransferase 1)	HBV (↓)	[35]
let-7 family	down	STAT3 (transcription factor)	HBV (↑?), HCC (↑)	[36]
		Viral targets		
miR-122	up	HBV DNA polymerase	HBV (↓)	[37]
miR-125a-5p	up	HBsAg (HBV surface antigen)	HBV (↓)	[38]
miR-199-3p	up	HBsAg	HBV (↓)	[39]
miR-210	up	HBV pre-S1 (pre-surface 1)	HBV (↓)	[39]

3.2. Role of miRNAs in the HBV Replication

The role of miRNAs in HBV replication is therefore dependent on the phase of HBV infection. During the acute phase, the virus must activate its replication while avoiding destruction by the immune system. During the chronic phase, the virus reaches a "dormant" state where the viral replication must be restricted and viral evasion maintained. This leads to a time-dependent intricate interaction network in which miRNAs play an important role.

One of the best studied miRNAs in HBV infection and other liver-related diseases is miR-122. This liver-specific miRNA is expressed at high levels in normal hepatocytes (about 70% of the total miRNA population in the adult liver) [40] and is pivotal in numerous aspects of the liver function such as lipid metabolism, liver development, differentiation, growth and neoplastic transformation [41]. While the loss of miR-122 expression impedes hepatitis C virus (HCV) replication [42], it enhances the replication in the circumstance of HBV infection [6]. However, miR-122 can negatively regulate the viral gene expression and replication by direct binding to a highly conserved sequence of HBV [37]. This repression effect can apparently be impeded by a negative feedback loop involving the Heme oxygenase-1 [43]. A recent study has reported the indirect implication of the HBV X protein (HBx) in miR-122 dysregulation [44] that could, at least partially, explain the difference observed between the two viruses.

Figure 2. Schematic representation of HBV life cycle. The virus infects a cell by an initial attachment to a cellular receptor that allows its internalization (step 1). In the cytoplasm, the virus is uncoated and the nucleocapsid is transported to the nuclear membrane (step 2). The viral genome is released into the nucleus under its relaxed circular form (rcDNA) and converted into a covalently closed circular DNA (cccDNA) from which all the viral RNAs are produced (steps 3 to 5). The viral RNAs transfer to the cytoplasm for traduction of the different viral proteins (steps 6 and 7) or for subsequent reverse transcription of the pregenomic RNA (pgRNA, steps 6, 8 and 9). All the viral components move to the proper place and assemble together to form new mature virions (steps 8, 10 and 11). The virus also produces non-infectious particles and extracellular antigen (HBeAg) as a decoy for the immune system of the host (step 12). The nucleocapsid containing the rcDNA and the HBV X protein (HBx) can go back to the nucleus in order to amplify the cccDNA and maintain the viral production.

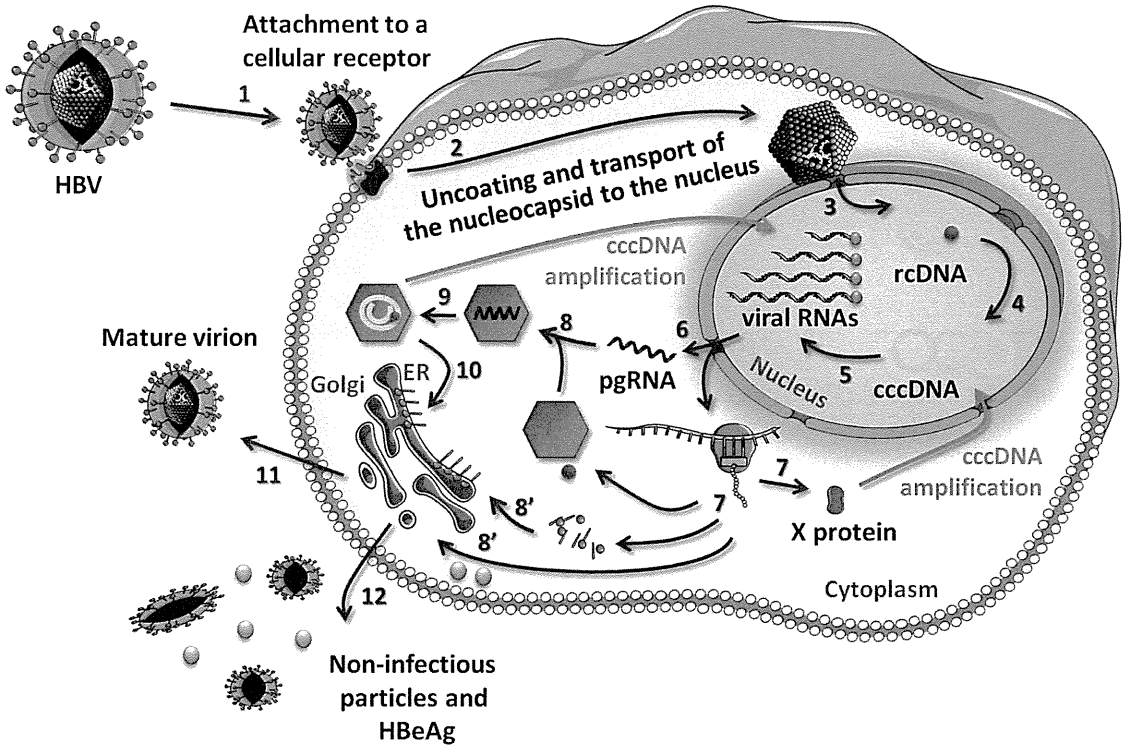

On the other hand, miR-1 can enhance the HBV core promoter transcription by down-regulating the expression of the histone deacetylase 4 (HDAC4) [45]. This miRNA might act complementary to the nuclear HBx in order to induce epigenetic modifications on the cccDNA and amplify the viral genome [45,46].

miR-372, together with miR-373, also supports HBV gene expression by targeting the nuclear factor I/B [47]. This cellular protein is known to be an important regulator of several viruses [48].

The let-7 family of miRNAs has been demonstrated to be negatively regulated by HBx [36]. The consequence of this down-regulation is the increase activity of the signal transducer and activator of transcription 3 (STAT3) that supports cell proliferation, and potentially viral replication and hepatocarcinogenesis.

Finally, miR-501 has been suggested to work with HBx for the benefit of viral replication [33]. HBx itself has also the ability to dysregulate the cellular miRNAs expression. This small protein is a key regulator of HBV infection. It is usually overexpressed in HCC and is involved in hepatocarcinogenesis [48].

3.3. Role of miRNAs in the Immune Evasion of HBV

miRNAs are important in the development and function of immune system [49]. In particular, miR-155 has multi-roles during innate immune response such as regulation of the acute inflammatory response after recognition of pathogens by the toll-like receptors [50,51]. Su and collaborators demonstrated that ectopic expression of miR-155 in human hepatoma cells could enhance the innate immunity through promotion of the janus kinase (JAK)/STAT pathway and down-regulate HBx expression [31].

On the other hand, a study analyzing the modified expression profiles of miRNAs in a stable HBV-expressing cell line revealed the upregulation of miR-181a [5]. The dysregulation of this miRNA in liver cell might participate to HBV replication through inhibition of the human leukocyte antigen A (HLA-A)-dependent HBV antigen presentation.

It is now unclear if the miRNAs altered in the infected hepatocytes, such as miR-181a and miR-146 [5], that have specific regulatory functions in the immune cells as well [49], could affect directly these cells to support viral evasion. The presence of circulating miRNAs and the existence of intercellular nanovesicle-mediated miRNA transfer that modulates the environment, could potentially support that hypothesis [52–57].

3.4. Role of miRNAs in the Establishment of HBV Chronic Infection

The natural history of HBV infection shows often a transition from acute to chronic infection, especially in young children. The virus reaches a "dormant" state into the infected hepatocytes, under the cccDNA form, and survive until its eventual life cycle reactivation [3,35,45,58]. One study reported the CpG islands methylation of the cccDNA by DNA methyltransferase 1 (DNMT1) to prevent the viral gene expression and therefore the viral antigen presentation. The DNMT1 overexpression is induced by a decrease of miR-152, under the effect of HBx [35].

miR-1 illustrates the duality of actions that can be observed in the course of HBV infection. As said previously, this miRNA can promote viral replication but it can also inhibit the cell proliferation and even induce a reverse cancer cell phenotype [28]. The effect on HCC was confirmed in another study [59].

Also, miR-122 can bind directly to the polymerase region in order to repress its expression [37]. Similar observations were made for miR-125a-5p, miR-199a-3p that can affect the S region and miR-210 that can affect the pre-S1 region [38,39]. Since the RNA intermediates of HBV (pgRNA and transcripts) are good targets of miRNA action, it is not surprising to observe several cellular miRNAs targeting them. However, it remains to be determined whether the targeting of HBV transcripts represents an active anti-viral mechanism of the host or if the virus has evolved to hijack these cellular miRNAs in order to reach its "dormant" state.

4. Role of miRNAs in HBV-Related Diseases

The modifications induced as a result of HBV infection profoundly alter the cellular and overall organism homeostasis. They are usually associated with diseases, including liver cirrhosis with fibrosis and HCC. The liver cirrhosis turns most of the time into HCC.

4.1. Role of miRNAs in HBV-Related Cirrhosis

Numerous studies have tried to identify and characterize the miRNAs involved in liver cirrhosis and therefore differently expressed during this intermediate phase. Roderburg et al. investigated the role of miRNAs in liver fibrosis on a carbon tetrachloride-induced hepatic fibrogenesis and bile-duct ligation mouse models [34]. They observed a significant down-regulation of all the members of the miR-29 family in the two models. The decreased expression was induced by the transforming growth factor beta (TGF-β), inflammatory signals and the nuclear factor kappa B (NFκB) pathways. miR-29c was also identified in another report focusing on the miRNA expression profile in patients with HCC-positive or HCC-negative chronic hepatitis B and hepatitis C virus [22] (Table 1).

Nevertheless, the global miRNA expression profile analysis of human liver tissues from different inflammation, infection and cancer states are not always consistent. It sometimes revealed a particular profile due to the association of both viral hepatitis and cirrhosis [60] or regarding to the type of viral hepatitis [22] and sometimes showed no difference [61]. Further experiments are therefore required to identify the exact molecular mechanisms implicating miRNAs and viral components in the development of cirrhosis and in the transition from cirrhosis to HCC in the patients with chronic viral hepatitis.

4.2. Role of miRNAs in HBV-Related HCC

When the cellular modifications and inflammation are too high and maintained for too long, the liver cirrhosis usually evolves into HCC.

The miR-17-92 cluster is important in the HBV infection and associated HCC. This polycistron includes six miRNAs (mir-17-5p, miR-18a, miR-19a, miR-19b, miR-20a and miR-92a-1) and its upregulated expression is associated with malignancies [62]. By using human HBV-positive human HCC tissues, hepatoma cell lines and woodchuck hepatitis virus-induced HCC animal model [63], Connolly and colleagues were able to demonstrate the elevated expression of miR-17-92 cluster and its implication in the malignant phenotype [29] (Table 1). The expression could be amplified by c-myc activation [64], under HBx control [65], to contribute to HBV latency state [66]. The consequence is the induction of liver oncogenesis.

Because of its role in immune response, miR-155 is also implicated in hepatocarcinogenesis. Indeed, its upregulation can lead to prolonged exposure to inflammation, a well-known causal agent to cancers like HCC [67]. Using HCC-induced mouse model, Wang and collaborators have demonstrated the oncogenic role of miR-155 at the early stages of the tumorigenesis [30] (Table 1).

To conclude, the liver-specific miR-122 has been extensively studied in the liver-associated diseases. Its expression is low in HCC tissues, including those with viral chronic hepatitis [6,68] (Table 1). As described in point 3.2, the regulation of miR-122 is very complex and helps either promotion or

inhibition of the HBV replication. In HCC cells, the "dormant" state of HBV implicates a replication rate very low or inexistent [69]. The recent data accumulate evidence of miR-122 as a highly potential linker between HBV infection and liver carcinogenesis [6,70]. Because of its characteristics, miR-122 is therefore a target of choice for future clinical applications.

5. miRNAs as Molecular Tools Against HBV Infection and HBV-Related Diseases

The significance of miRNAs in viral replication, antiviral immunity and liver carcinogenesis emphasizes their values as diagnostic, prognostic and therapeutic targets for HBV infection and HBV-induced diseases.

miR-122 and miR-18a are of particular interest for diagnostic and/or prognostic applications. They are both released in the blood and could be used as potential non-invasive biomarkers for HBV-related HCC screening [5,53,54]. Some other reports suggest the use of a miRNA panel in order to improve the specificity of the test [55,56]. In addition with the current routinely used markers such as HBV surface antigen (HBsAg), HBV extracellular antigen (HbeAg) and alanine aminotransferase (ALT), the circulating miRNAs represent a significant clinical value for better evaluation of the HBV-infection status, liver injury and early diagnosis of HCC.

In the therapeutic perspective, the liver cirrhosis is an event prior to HCC development and being able to interfere with this process would prevent carcinogenesis. For example, a strategy based on administration of miR-29 mimic might prevent liver fibrosis (Section 4.1) [34]. However, the disease is often discovered when hepatocarcinogenesis has already developed and HCC does not always show underlying cirrhosis [71]. Finding therapeutic targets involved in HCC is thus a major issue.

For this purpose, the work of Ura's group is valuable [22]. They analyzed the livers of HBV and HCV positive patients with HCC to identify the miRNAs that are differentially expressed. Nineteen miRNAs were clearly differentiated between HBV and HCV groups, six specific for HBV and thirteen specific for HCV. Based on the miRNAs profile, they made a pathway analysis of candidate targeted genes and were also able to distinguish the cellular mechanisms altered in HBV or HCV-infected livers. The HBV infection alters mostly the pathways related to signal transduction, inflammation and natural killer toxicity, DNA damage, recombination, and cell death, while HCV infection modifies those involved in immune response involving antigen presentation, cell cycle and cell adhesion. Although very interesting, their results are not consistent with those presented in other reports [60,61] and confirmation of the targets needs to be done before considering their clinical application.

Finally, technological advances in the delivery of miRNA and RNA interference enable safe and efficient *in vivo* miRNA gene therapy, as exemplify by the recent study from Kota and colleagues on the liver cancer [72]. They used an adeno-associated virus to deliver miR-26a in a mouse model of HCC. This resulted in the successful inhibition of the cancer cell proliferation, induction of the tumor-specific apoptosis, and protection from disease progression without toxicity.

6. Conclusions

miRNAs have emerged as new key players in the control of gene expression in cells. Investigations of their profiling have unveiled specific miRNA dysregulations in tumors and during viral infection.

The HBV is a widespread pathogen that is implicated in HCC development. Numerous cellular miRNAs interacting with HBV have been identified. They reflect the cellular pathways that are altered as a result of the viral infection, viral infection that triggers the liver cirrhosis and carcinogenesis as side effects. On the viral point of view, the dysregulated pathways mirror the strategies of the virus to allow its replication and evade the host defense mechanisms to survive. On the cellular point of view, they mirror the immune response that tries to get rid of the intruder and that becomes dysregulated. The present and future knowledge about the interaction between miRNA, HBV infection and HCC development and progress will probably allow developing strategies and tools to cope, efficiently and at various steps, with the liver carcinogenesis induced by HBV infection.

Acknowledgments

This work was supported in part by a grant-in-aid for the Third-Term Comprehensive 10-Year Strategy for Cancer Control of Japan; Project for Development of Innovative Research on Cancer Therapeutics (P-Direct); Scientific Research on Priority Areas Cancer from the Japanese Ministry of Education, Culture, Sports, Science, and Technology; and the Program for Promotion of Fundamental Studies in Health Sciences of the National Institute of Biomedical Innovation of Japan. The authors would like to thank Servier Medical Art for their image bank used to create the illustrations.

Conflicts of Interest

The authors declare no conflict of interest.

References

1. Bartel, D.P. MicroRNAs: Target recognition and regulatory functions. *Cell* **2009**, *136*, 215–233.
2. Skalsky, R.L.; Cullen, B.R. Viruses, microRNAs, and host interactions. *Annu. Rev. Microbiol.* **2010**, *64*, 123–141.
3. Ganem, D.; Prince, A.M. Hepatitis B virus infection—Natural history and clinical consequences. *N. Engl. J. Med.* **2004**, *350*, 1118–1129.
4. Parkin, D.M. The global health burden of infection-associated cancers in the year 2002. *Int. J. Cancer* **2006**, *118*, 3030–3044.
5. Liu, Y.; Zhao, J.J.; Wang, C.M.; Li, M.Y.; Han, P.; Wang, L.; Cheng, Y.Q.; Zoulim, F.; Ma, X.; Xu, D.P. Altered expression profiles of microRNAs in a stable hepatitis B virus-expressing cell line. *Chin. Med. J.* **2009**, *122*, 10–14.
6. Wang, S.; Qiu, L.; Yan, X.; Jin, W.; Wang, Y.; Chen, L.; Wu, E.; Ye, X.; Gao, G.F.; Wang, F.; *et al.* Loss of microRNA 122 expression in patients with hepatitis B enhances hepatitis B virus replication through cyclin G(1)-modulated P53 activity. *Hepatology* **2012**, *55*, 730–741.
7. He, L.; Hannon, G.J. MicroRNAs: Small RNAs with a big role in gene regulation. *Nat. Rev. Genet.* **2004**, *5*, 522–531.
8. Vasudevan, S.; Tong, Y.; Steitz, J.A. Switching from repression to activation: Micrornas can up-regulate translation. *Science* **2007**, *318*, 1931–1934.

9. Eiring, A.M.; Harb, J.G.; Neviani, P.; Garton, C.; Oaks, J.J.; Spizzo, R.; Liu, S.; Schwind, S.; Santhanam, R.; Hickey, C.J.; *et al.* miR-328 functions as an RNA decoy to modulate hnRNP E2 regulation of mRNA translation in leukemic blasts. *Cell* **2010**, *140*, 652–665.
10. Gonzalez, S.; Pisano, D.G.; Serrano, M. Mechanistic principles of chromatin remodeling guided by siRNAs and miRNAs. *Cell Cycle* **2008**, *7*, 2601–2608.
11. Kim, D.H.; Saetrom, P.; Snove, O., Jr.; Rossi, J.J. MicroRNA-directed transcriptional gene silencing in mammalian cells. *Proc. Natl. Acad. Sci. USA* **2008**, *105*, 16230–16235.
12. Lim, L.P.; Lau, N.C.; Garrett-Engele, P.; Grimson, A.; Schelter, J.M.; Castle, J.; Bartel, D.P.; Linsley, P.S.; Johnson, J.M. Microarray analysis shows that some microRNAs downregulate large numbers of target mRNAs. *Nature* **2005**, *433*, 769–773.
13. Ambros, V. The functions of animal microRNAs. *Nature* **2004**, *431*, 350–355.
14. Baek, D.; Villen, J.; Shin, C.; Camargo, F.D.; Gygi, S.P.; Bartel, D.P. The impact of microRNAs on protein output. *Nature* **2008**, *455*, 64–71.
15. Lee, I.; Ajay, S.S.; Yook, J.I.; Kim, H.S.; Hong, S.H.; Kim, N.H.; Dhanasekaran, S.M.; Chinnaiyan, A.M.; Athey, B.D. New class of microRNA targets containing simultaneous 5'-UTR and 3'-UTR interaction sites. *Genome Res.* **2009**, *19*, 1175–1183.
16. Calin, G.A.; Sevignani, C.; Dumitru, C.D.; Hyslop, T.; Noch, E.; Yendamuri, S.; Shimizu, M.; Rattan, S.; Bullrich, F.; Negrini, M.; Croce, C.M. Human microRNA genes are frequently located at fragile sites and genomic regions involved in cancers. *Proc. Natl. Acad. Sci. USA* **2004**, *101*, 2999–3004.
17. Calin, G.A.; Ferracin, M.; Cimmino, A.; di Leva, G.; Shimizu, M.; Wojcik, S.E.; Iorio, M.V.; Visone, R.; Sever, N.I.; Fabbri, M.; *et al.* A MicroRNA signature associated with prognosis and progression in chronic lymphocytic leukemia. *N. Engl. J. Med.* **2005**, *353*, 1793–1801.
18. Bi, Y.; Liu, G.; Yang, R. MicroRNAs: Novel regulators during the immune response. *J. Cell Physiol.* **2009**, *218*, 467–472.
19. Fasseu, M.; Treton, X.; Guichard, C.; Pedruzzi, E.; Cazals-Hatem, D.; Richard, C.; Aparicio, T.; Daniel, F.; Soule, J. C.; Moreau, R.; *et al.* Identification of restricted subsets of mature microRNA abnormally expressed in inactive colonic mucosa of patients with inflammatory bowel disease. *PLoS One* **2010**, *5*, doi:10.1371/journal.pone.0013160.
20. Sethi, P.; Lukiw, W.J. Micro-RNA abundance and stability in human brain: Specific alterations in Alzheimer's disease temporal lobe neocortex. *Neurosci. Lett.* **2009**, *459*, 100–104.
21. Latronico, M.V.; Catalucci, D.; Condorelli, G. Emerging role of microRNAs in cardiovascular biology. *Circ. Res.* **2007**, *101*, 1225–1236.
22. Ura, S.; Honda, M.; Yamashita, T.; Ueda, T.; Takatori, H.; Nishino, R.; Sunakozaka, H.; Sakai, Y.; Horimoto, K.; Kaneko, S. Differential microRNA expression between hepatitis B and hepatitis C leading disease progression to hepatocellular carcinoma. *Hepatology* **2009**, *49*, 1098–1112.
23. Jin, W.B.; Wu, F.L.; Kong, D.; Guo, A.G. HBV-encoded microRNA candidate and its target. *Comput. Biol. Chem.* **2007**, *31*, 124–126.
24. Seeger, C.; Mason, W.S. Hepatitis B virus biology. *Microbiol. Mol. Biol. Rev.* **2000**, *64*, 51–68.
25. Yan, H.; Zhong, G.; Xu, G.; He, W.; Jing, Z.; Gao, Z.; Huang, Y.; Qi, Y.; Peng, B.; Wang, H.; *et al.* Sodium taurocholate cotransporting polypeptide is a functional receptor for human hepatitis B and D virus. *Elife* **2012**, *1*, e00049.

26. Brechot, C.; Pourcel, C.; Louise, A.; Rain, B.; Tiollais, P. Presence of integrated hepatitis B virus DNA sequences in cellular DNA of human hepatocellular carcinoma. *Nature* **1980**, *286*, 533–535.
27. Paterlini-Brechot, P.; Saigo, K.; Murakami, Y.; Chami, M.; Gozuacik, D.; Mugnier, C.; Lagorce, D.; Brechot, C. Hepatitis B virus-related insertional mutagenesis occurs frequently in human liver cancers and recurrently targets human telomerase gene. *Oncogene* **2003**, *22*, 3911–3916.
28. Zhang, X.; Zhang, E.; Ma, Z.; Pei, R.; Jiang, M.; Schlaak, J.F.; Roggendorf, M.; Lu, M. Modulation of hepatitis B virus replication and hepatocyte differentiation by MicroRNA-1. *Hepatology* **2011**, *53*, 1476–1485.
29. Connolly, E.; Melegari, M.; Landgraf, P.; Tchaikovskaya, T.; Tennant, B.C.; Slagle, B.L.; Rogler, L.E.; Zavolan, M.; Tuschl, T.; Rogler, C.E. Elevated expression of the miR-17-92 polycistron and miR-21 in hepadnavirus-associated hepatocellular carcinoma contributes to the malignant phenotype. *Am. J. Pathol.* **2008**, *173*, 856–864.
30. Wang, B.; Majumder, S.; Nuovo, G.; Kutay, H.; Volinia, S.; Patel, T.; Schmittgen, T.D.; Croce, C.; Ghoshal, K.; Jacob, S.T. Role of microRNA-155 at early stages of hepatocarcinogenesis induced by choline-deficient and amino acid-defined diet in C57BL/6 mice. *Hepatology* **2009**, *50*, 1152–1161.
31. Su, C.; Hou, Z.; Zhang, C.; Tian, Z.; Zhang, J. Ectopic expression of microRNA-155 enhances innate antiviral immunity against HBV infection in human hepatoma cells. *Virol. J.* **2011**, *8*, doi:10.1186/1743-422X-8-354.
32. Guo, H.; Liu, H.; Mitchelson, K.; Rao, H.; Luo, M.; Xie, L.; Sun, Y.; Zhang, L.; Lu, Y.; Liu, R.; *et al.* MicroRNAs-372/373 promote the expression of hepatitis B virus through the targeting of nuclear factor I/B. *Hepatology* **2011**, *54*, 808–819.
33. Jin, J.; Tang, S.; Xia, L.; Du, R.; Xie, H.; Song, J.; Fan, R.; Bi, Q.; Chen, Z.; Yang, G.; *et al.* MicroRNA-501 promotes HBV replication by targeting HBXIP. *Biochem. Biophys. Res. Commun.* **2013**, *430*, 1228–1233.
34. Roderburg, C.; Urban, G.W.; Bettermann, K.; Vucur, M.; Zimmermann, H.; Schmidt, S.; Janssen, J.; Koppe, C.; Knolle, P.; Castoldi, M.; *et al.* Micro-RNA profiling reveals a role for miR-29 in human and murine liver fibrosis. *Hepatology* **2010**, *53*, 209–218.
35. Huang, J.; Wang, Y.; Guo, Y.; Sun, S. Down-regulated microRNA-152 induces aberrant DNA methylation in hepatitis B virus-related hepatocellular carcinoma by targeting DNA methyltransferase 1. *Hepatology* **2010**, *52*, 60–70.
36. Wang, Y.; Lu, Y.; Toh, S.T.; Sung, W.K.; Tan, P.; Chow, P.; Chung, A.Y.; Jooi, L.L.; Lee, C.G. Lethal-7 is down-regulated by the hepatitis B virus x protein and targets signal transducer and activator of transcription 3. *J. Hepatol.* **2010**, *53*, 57–66.
37. Chen, Y.; Shen, A.; Rider, P.J.; Yu, Y.; Wu, K.; Mu, Y.; Hao, Q.; Liu, Y.; Gong, H.; Zhu, Y.; *et al.* A liver-specific microRNA binds to a highly conserved RNA sequence of hepatitis B virus and negatively regulates viral gene expression and replication. *FASEB J.* **2011**, *25*, 4511–4521.
38. Potenza, N.; Papa, U.; Mosca, N.; Zerbini, F.; Nobile, V.; Russo, A. Human microRNA hsa-miR-125a-5p interferes with expression of hepatitis B virus surface antigen. *Nucleic Acids Res.* **2011**, *39*, 5157–5163.
39. Zhang, G.L.; Li, Y.X.; Zheng, S.Q.; Liu, M.; Li, X.; Tang, H. Suppression of hepatitis B virus replication by microRNA-199a-3p and microRNA-210. *Antiviral Res.* **2010**, *88*, 169–175.

40. Lagos-Quintana, M.; Rauhut, R.; Yalcin, A.; Meyer, J.; Lendeckel, W.; Tuschl, T. Identification of tissue-specific microRNAs from mouse. *Curr. Biol.* **2002**, *12*, 735–739.
41. Girard, M.; Jacquemin, E.; Munnich, A.; Lyonnet, S.; Henrion-Caude, A. miR-122, a paradigm for the role of microRNAs in the liver. *J. Hepatol.* **2008**, *48*, 648–656.
42. Jopling, C.L.; Yi, M.; Lancaster, A.M.; Lemon, S.M.; Sarnow, P. Modulation of hepatitis C virus RNA abundance by a liver-specific MicroRNA. *Science* **2005**, *309*, 1577–1581.
43. Qiu, L.; Fan, H.; Jin, W.; Zhao, B.; Wang, Y.; Ju, Y.; Chen, L.; Chen, Y.; Duan, Z.; Meng, S. miR-122-induced down-regulation of HO-1 negatively affects miR-122-mediated suppression of HBV. *Biochem. Biophys. Res. Commun.* **2010**, *398*, 771–777.
44. Song, K.; Han, C.; Zhang, J.; Lu, D.; Dash, S.; Feitelson, M.; Lim, K.; Wu, T. Epigenetic regulation of miR-122 by PPARgamma and hepatitis B virus X protein in hepatocellular carcinoma cells. *Hepatology* **2013**, doi: 10.1002/hep.26514.
45. Belloni, L.; Pollicino, T.; de Nicola, F.; Guerrieri, F.; Raffa, G.; Fanciulli, M.; Raimondo, G.; Levrero, M. Nuclear HBx binds the HBV minichromosome and modifies the epigenetic regulation of cccDNA function. *Proc. Natl. Acad. Sci. USA* **2009**, *106*, 19975–19979.
46. Pollicino, T.; Belloni, L.; Raffa, G.; Pediconi, N.; Squadrito, G.; Raimondo, G.; Levrero, M. Hepatitis B virus replication is regulated by the acetylation status of hepatitis B virus cccDNA-bound H3 and H4 histones. *Gastroenterology* **2006**, *130*, 823–837.
47. Nagata, K.; Guggenheimer, R.A.; Hurwitz, J. Specific binding of a cellular DNA replication protein to the origin of replication of adenovirus DNA. *Proc. Natl. Acad. Sci. USA* **1983**, *80*, 6177–6181.
48. Tian, Y.; Yang, W.; Song, J.; Wu, Y.; Ni, B. HBV X protein-induced aberrant epigenetic modifications contributing to human hepatocellular carcinoma pathogenesis. *Mol. Cell. Biol.* **2013**, *33*, 2810–2816.
49. Baltimore, D.; Boldin, M.P.; O'Connell, R.M.; Rao, D.S.; Taganov, K.D. MicroRNAs: New regulators of immune cell development and function. *Nat. Immunol.* **2008**, *9*, 839–845.
50. O'Connell, R.M.; Taganov, K.D.; Boldin, M.P.; Cheng, G.; Baltimore, D. MicroRNA-155 is induced during the macrophage inflammatory response. *Proc. Natl. Acad. Sci. USA* **2007**, *104*, 1604–1609.
51. Tili, E.; Michaille, J.J.; Cimino, A.; Costinean, S.; Dumitru, C.D.; Adair, B.; Fabbri, M.; Alder, H.; Liu, C.G.; Calin, G.A.; Croce, C.M. Modulation of miR-155 and miR-125b levels following lipopolysaccharide/TNF-alpha stimulation and their possible roles in regulating the response to endotoxin shock. *J. Immunol.* **2007**, *179*, 5082–5089.
52. Arataki, K.; Hayes, C.N.; Akamatsu, S.; Akiyama, R.; Abe, H.; Tsuge, M.; Miki, D.; Ochi, H.; Hiraga, N.; Imamura, M.; *et al.* Circulating microRNA-22 correlates with microRNA-122 and represents viral replication and liver injury in patients with chronic hepatitis B. *J. Med. Virol.* **2013**, *85*, 789–798.
53. Waidmann, O.; Bihrer, V.; Pleli, T.; Farnik, H.; Berger, A.; Zeuzem, S.; Kronenberger, B.; Piiper, A. Serum microRNA-122 levels in different groups of patients with chronic hepatitis B virus infection. *J. Viral Hepat.* **2012**, *19*, e58–e65.
54. Li, L.; Guo, Z.; Wang, J.; Mao, Y.; Gao, Q. Serum miR-18a: A potential marker for hepatitis B virus-related hepatocellular carcinoma screening. *Dig. Dis. Sci.* **2012**, *57*, 2910–2916.

55. Li, L.M.; Hu, Z.B.; Zhou, Z.X.; Chen, X.; Liu, F.Y.; Zhang, J.F.; Shen, H.B.; Zhang, C.Y.; Zen, K. Serum microRNA profiles serve as novel biomarkers for HBV infection and diagnosis of HBV-positive hepatocarcinoma. *Cancer Res.* **2010**, *70*, 9798–9807.
56. Zhou, J.; Yu, L.; Gao, X.; Hu, J.; Wang, J.; Dai, Z.; Wang, J.F.; Zhang, Z.; Lu, S.; Huang, X.; *et al.* Plasma microRNA panel to diagnose hepatitis B virus-related hepatocellular carcinoma. *J. Clin. Oncol.* **2011**, *29*, 4781–4788.
57. Kogure, T.; Lin, W.L.; Yan, I.K.; Braconi, C.; Patel, T. Intercellular nanovesicle-mediated microRNA transfer: A mechanism of environmental modulation of hepatocellular cancer cell growth. *Hepatology* **2011**, *54*, 1237–1248.
58. Belloni, L.; Allweiss, L.; Guerrieri, F.; Pediconi, N.; Volz, T.; Pollicino, T.; Petersen, J.; Raimondo, G.; Dandri, M.; Levrero, M. IFN-alpha inhibits HBV transcription and replication in cell culture and in humanized mice by targeting the epigenetic regulation of the nuclear cccDNA minichromosome. *J. Clin. Invest.* **2012**, *122*, 529–537.
59. Datta, J.; Kutay, H.; Nasser, M.W.; Nuovo, G.J.; Wang, B.; Majumder, S.; Liu, C.G.; Volinia, S.; Croce, C.M.; Schmittgen, T.D.; *et al.* Methylation mediated silencing of MicroRNA-1 gene and its role in hepatocellular carcinogenesis. *Cancer Res.* **2008**, *68*, 5049–5058.
60. Jiang, J.; Gusev, Y.; Aderca, I.; Mettler, T.A.; Nagorney, D.M.; Brackett, D.J.; Roberts, L.R.; Schmittgen, T.D. Association of MicroRNA expression in hepatocellular carcinomas with hepatitis infection, cirrhosis, and patient survival. *Clin. Cancer Res.* **2008**, *14*, 419–427.
61. Murakami, Y.; Yasuda, T.; Saigo, K.; Urashima, T.; Toyoda, H.; Okanoue, T.; Shimotohno, K. Comprehensive analysis of microRNA expression patterns in hepatocellular carcinoma and non-tumorous tissues. *Oncogene* **2006**, *25*, 2537–2545.
62. Hayashita, Y.; Osada, H.; Tatematsu, Y.; Yamada, H.; Yanagisawa, K.; Tomida, S.; Yatabe, Y.; Kawahara, K.; Sekido, Y.; Takahashi, T. A polycistronic microRNA cluster, miR-17-92, is overexpressed in human lung cancers and enhances cell proliferation. *Cancer Res.* **2005**, *65*, 9628–9632.
63. Popper, H.; Roth, L.; Purcell, R.H.; Tennant, B.C.; Gerin, J.L. Hepatocarcinogenicity of the woodchuck hepatitis virus. *Proc. Natl. Acad. Sci. USA* **1987**, *84*, 866–870.
64. He, L.; Thomson, J.M.; Hemann, M.T.; Hernando-Monge, E.; Mu, D.; Goodson, S.; Powers, S.; Cordon-Cardo, C.; Lowe, S.W.; Hannon, G.J.; *et al.* A microRNA polycistron as a potential human oncogene. *Nature* **2005**, *435*, 828–833.
65. Terradillos, O.; Billet, O.; Renard, C.A.; Levy, R.; Molina, T.; Briand, P.; Buendia, M.A. The hepatitis B virus X gene potentiates c-myc-induced liver oncogenesis in transgenic mice. *Oncogene* **1997**, *14*, 395–404.
66. Jung, Y.J.; Kim, J.W.; Park, S.J.; Min, B.Y.; Jang, E.S.; Kim, N.Y.; Jeong, S.H.; Shin, C.M.; Lee, S.H.; Park, Y.S.; *et al.* c-Myc-mediated overexpression of miR-17-92 suppresses replication of hepatitis B virus in human hepatoma cells. *J. Med. Virol.* **2013**, *85*, 969–978.
67. Berasain, C.; Castillo, J.; Perugorria, M.J.; Latasa, M.U.; Prieto, J.; Avila, M.A. Inflammation and liver cancer: new molecular links. *Ann. NY Acad. Sci.* **2009**, *1155*, 206–221.
68. Kutay, H.; Bai, S.; Datta, J.; Motiwala, T.; Pogribny, I.; Frankel, W.; Jacob, S.T.; Ghoshal, K. Downregulation of miR-122 in the rodent and human hepatocellular carcinomas. *J. Cell Biochem.* **2006**, *99*, 671–678.

69. Wong, D.K.; Yuen, M.F.; Poon, R.T.; Yuen, J.C.; Fung, J.; Lai, C.L. Quantification of hepatitis B virus covalently closed circular DNA in patients with hepatocellular carcinoma. *J. Hepatol.* **2006**, *45*, 553–559.
70. Fan, C.G.; Wang, C.M.; Tian, C.; Wang, Y.; Li, L.; Sun, W.S.; Li, R.F.; Liu, Y.G. miR-122 inhibits viral replication and cell proliferation in hepatitis B virus-related hepatocellular carcinoma and targets NDRG3. *Oncol. Rep.* **2011**, *26*, 1281–1286.
71. La Vecchia, C.; Lucchini, F.; Franceschi, S.; Negri, E.; Levi, F. Trends in mortality from primary liver cancer in Europe. *Eur. J. Cancer* **2000**, *36*, 909–915.
72. Kota, J.; Chivukula, R.R.; O'Donnell, K.A.; Wentzel, E.A.; Montgomery, C.L.; Hwang, H.W.; Chang, T.C.; Vivekanandan, P.; Torbenson, M.; Clark, K.R.; *et al.* Therapeutic microRNA delivery suppresses tumorigenesis in a murine liver cancer model. *Cell* **2009**, *137*, 1005–1017.

The Journal of Antibiotics (2013), 1–3

www.nature.com/ja

NOTE

Pyrrolizilactone, a new pyrrolizidinone metabolite produced by a fungus

Toshihiko Nogawa[1], Makoto Kawatani[2], Masakazu Uramoto[2], Akiko Okano[1], Harumi Aono[2], Yushi Futamura[2], Hiroyuki Koshino[3], Shunji Takahashi[4] and Hiroyuki Osada[1,2]

The Journal of Antibiotics advance online publication, 29 May 2013; doi:10.1038/ja.2013.55

Keywords: cytotoxicity; fungal metabolite; isolation; pyrrolizidinone; structure elucidation

In the course of our screening program to find structurally unique metabolites from microorganisms on the basis of spectral data collected through LC/MS analysis, a new pyrrolizidinone metabolite, pyrrolizilactone (**1**) (Figure 1), was discovered and isolated from an uncharacterized fungus. The structure of **1** was determined from spectroscopic results. Compound **1** showed moderate cytotoxic activity against HL-60 and HeLa cells.

Microorganisms have a tremendous capacity for producing structurally diverse metabolites, which show various activities.[1] They are important sources of pharmaceutical leads and therapeutic agents,[2,3] and are also used as bioprobes in chemical biology for the exploration of biological functions.[4,5] To search for and discover such structurally unique metabolites efficiently and rapidly, we have constructed a microbial metabolite fraction library with a spectral database on the basis of photodiode array detector-attached LC/MS analysis.[6,7] Through our methodology for the construction of this fraction library, we discovered and identified a 16-membered macrolactam with an unusual β-keto-amide moiety, verticilactam,[8] 6,6-spiroacetal polyketide, spirotoamides, A and B,[9] the new fraquinocins, I and J,[10] and 6-dimethylallylindole-3-carbaldehyde.[11] These results demonstrate the advantage of the fraction library in isolating novel metabolites from natural sources. We report herein the isolation of a novel compound from a fungi fraction library.

An 18-liter culture broth of an uncharacterized fungus was cultivated to obtain 16.1 g of an ethyl acetate-soluble extract. This was separated into eight fractions through a silica-gel column chromatography, with a stepwise gradient of $CHCl_3$/MeOH. The second fraction eluted with $CHCl_3$/MeOH (100:1) was further separated by chromatography using a Sephadex LH-20 column with $CHCl_3$/MeOH (1:1) to afford three fractions. The second fraction, showing an unidentified peak in LC/MS analysis, was purified by C_{18}-HPLC to afford a colorless amorphous solid (**1**, 5.5 mg). Colorless amorphous; $[\alpha]_{589}^{26} + 5.9°$ (*c* 0.08, MeOH); UV (MeOH) λ_{max} (log ε) 209 (3.34), 236 (3.01) nm; IR (ATR) ν_{max} (cm^{-1}) 3410, 2920, 2875, 1790, 1715, 1685, 1575, 1450, 1375, 1335, 1280, 1160, 1110, 1020; ^1H NMR and ^{13}C NMR data, see Table 1; HRESIMS *m/z*: 416.2433 $[M+H]^+$ (calcd for $C_{24}H_{34}NO_5$: 416.2437).

Compound **1** had the molecular formula $C_{24}H_{33}NO_5$, as determined by HRESIMS. The IR spectrum implied the presence of hydroxyl (3410 cm^{-1}) and carbonyl (1685, 1715 and 1790 cm^{-1}) groups. The ^1H NMR spectrum showed five methyl signals, which included a singlet, three doublets and a doublet of doublet (1.71 p.p.m., dd, $J = 0.9$, 0.9 Hz) branched at an sp^2 carbon, and an olefin signal (5.12 p.p.m., br s), suggesting that **1** contained a double bond (Supplementary Figure S1). The ^{13}C NMR spectrum showed 24 signals including five methyls, four methylenes, nine methines (including oxygenated and olefin carbons: 81.6 and 131.3 p.p.m.),

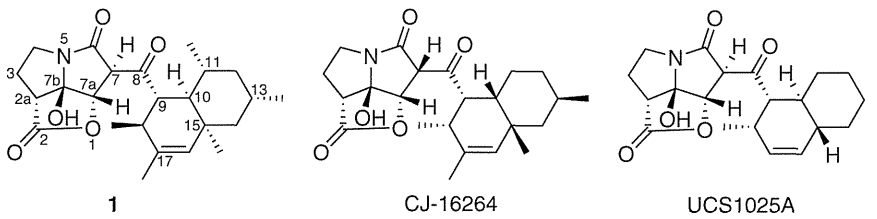

Figure 1 Structures of compound **1** and related compounds.

[1]Chemical Biology Research Group, RIKEN CSRS, Saitama, Japan; [2]Antibiotics Laboratory, RIKEN, Saitama, Japan; [3]RIKEN Global Research Cluster, RIKEN, Saitama, Japan and [4]Natural Product Biosynthesis Research Unit, RIKEN CSRS, Saitama, Japan
Correspondence: Dr H Osada, Antibiotics Laboratory, RIKEN, 2-1 Hirosawa, Wako, Saitama 351-0198, Japan.
E-mail: hisyo@riken.jp
Received 9 April 2013; revised 1 May 2013; accepted 7 May 2013

Table 1 ^{1}H and ^{13}C NMR chemical shifts with HMBC and NOESY correlations in $CDCl_3$

position	δ_C	δ_H*(Multiplicity, J in Hz)*	*HMBC*	*NOESY*
2	174.6	—	—	
2a	47.6	3.24 (dd, 9.2, 1.8)	C-2, 3, 4, 7b	H-3a, H-3b
3	29.9	2.73 a (dddd, 14.2, 9.6, 5.0, 1.8)	C-2, 2a, 9	—
		2.56 b (m)	C-2, 2a	—
4	41.8	3.82 a (ddd, 11.9, 9.6, 5.5)	—	H-3b
		3.35 b (ddd, 11.9, 9.6, 5.0)	C-3, 7b	H-3a
6	167.6	—	—	
7	63.1	4.15 (s)	C-6, 7a, 7b, 8	H-9, H-18
7a	81.6	4.65 (s)	C-2, 6, 7, 7b, 8	H-2a, H-7, H-9
7b	100.7	—	—	
8	210.3	—	—	
9	58.8	2.85 (br s)	C-8, 10, 11, 17, 18, Me-18	H-10, Me-11, Me-18
10	46.2	2.10 ax. (br d, 10.5)	C-8, 9, 11, 15, 16, 18, Me-11	H-12ax, H-14ax, Me-11, Me-15
11	32.9	1.57 ax. (m)	—	Me-11, Me-18
12	44.4	0.78 ax. (br ddd, 12.4, 11.5, 11.5)	—	—
		1.61 eq. (ddd, 12.4, 3.2, 3.2)	—	Me-13
13	28.3	1.43 ax. (m)	—	Me-13
14	50.3	0.98 ax. (dd, 12.4, 12.4)	C-12, 15, 16, Me-15	Me-13, Me-15
		1.40 eq. (dd, 12.4, 2.7)	—	Me-13, Me-15
15	37.5	—	—	
16	131.3	5.12 (br s)	C-10, 14, Me-15, Me-17	H-14eq, Me-15, Me-17
17	133.0	—	—	
18	29.4	2.93 (m)	C-8, 17, Me-18	Me-15, Me-17, Me-18
Me-11	21.0	1.04 (3H, d, 6.4)	C-10, 11, 12	—
Me-13	22.3	0.81 (3H, d, 6.4)	C-12, 13, 14	—
Me-15	29.8	0.62 (3H, s)	C-10, 14, 15, 16	—
Me-17	21.7	1.71 (3H, dd, 0.9, 0.9)	C-17, 18	—
Me-18	21.2	1.11 (3H, d, 7.8)	C-9, 17, 18	—

^{1}H and ^{13}C NMR spectra were recorded at 500 and 125 MHz, respectively.

and six quaternary carbons including an olefin carbon (133.0 p.p.m.) and three carbonyl ones (167.6, 174.6 and 210.3 p.p.m.), one of which was a ketone (Supplementary Figure S2). These were confirmed by the ^{13}C DEPT experiment and HSQC spectrum (Supplementary Figures S3 and S4). The spectrum also included an unusual quaternary carbon at 100.7 p.p.m., implied to bear both oxygen and nitrogen atoms or two oxygen atoms. These data and the index of hydrogen deficiency of nine suggested that compound **1** consisted of a five-ring system with three carbonyls and one double bond. The planar structure was established through the interpretation of the 2D NMR spectra (Figure 2a). The connections between protons and carbons were confirmed by correlations in the HSQC spectrum. Two proton-spin systems from H-2a to H-4 and from Me-18 to H-14 with methyl branches at C-11 and C-13 were constructed from the correlations in the DQF-COSY and HSQC-TOCSY spectra (Supplementary Figures S5 and S6). The overall structure was established from the long-range correlations in the HMBC spectrum (Supplementary Figure S7). The HMBC correlations from Me-15 to C-10, C-14, C-15 and C-16 showed the attachment of Me-15 at C-15, which was connected to C-10 to construct a cyclohexane substructure, and connectivities from C-14 to C-16. These were confirmed by the HMBC correlations from H-10 to C-15 and C-16, and from H-14 to C-15 and C-16. Me-17, which should be branched at an sp^2 carbon, showed HMBC correlations to C-16, C-17 and C-18, suggesting a methyl branch at C-17 and connectivities from C-16 to C-18. These results in combination with the DQF-COSY result indicated a pentamethyl-octahydronaphthalene structure; this was confirmed by HMBC correlations from H-9 to C-15 and C-17, and from both H-18 and Me-18 to C-17.

A pyrrolizidinone moiety fused with γ-lactone system was confirmed by HMBC correlations and NMR chemical shift values with the consideration of the index of hydrogen deficiency, which suggested the remaining substructure required a three-ring system. The HMBC correlations from H-2a and H-3 to a carbonyl carbon C-2 and from H-2a to C-7b having the unusual ^{13}C NMR chemical shift value of 100.7 p.p.m. were observed. The C-7b was also correlated from H-7 and H-7a in the HMBC spectrum, both of which showed HMBC correlations to another carbonyl carbon C-6. These HMBC correlations and the connectivities from H-2a to H-4 was confirmed by DQF-COSY, as described above, were allowing the connectivities between C-4 and C-6 with a branch of the carbonyl carbon C-2 at C-2a position. The connection between C-7 and C-7a, both of which were observed as a singlet signal in the ^{1}H NMR spectrum and did not show COSY correlation, was confirmed by an HMBC correlation from H-7 to C-7a and NOE between H-7 and H-7a in the phase-sensitive NOESY spectrum (Supplementary Figure S8). An HMBC correlation from H-7a to C-2 implied the presence of a ring system, and it was confirmed as a γ-lactone by the ^{13}C NMR chemical shift values of C-2 and C-7a (174.6 and 81.6 p.p.m., respectively). Based on the above results and the consideration of molecular formula, the C-7b was supposed to have both oxygen and nitrogen atoms. The ^{13}C NMR chemical shift values of C-4 and C-6 (41.8 and 167.6 p.p.m., respectively) and the substructure being a tricyclo-system allowed the construction of a pyrrolizidinone skeleton, which were also confirmed by an HMBC correlation from H-4 to C-7b. The pyrrolizidinone substructure was connected to the decalin moiety through the ketone C-8, which was confirmed by HMBC correlations from H-7, H-7a,

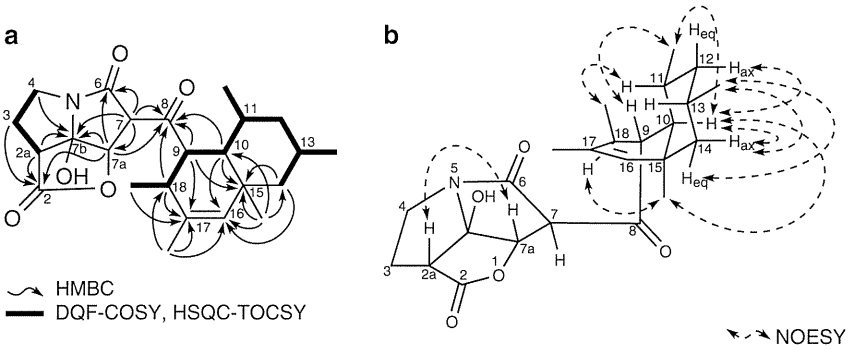

Figure 2 Selected DQF-COSY and HMBC correlations (**a**) and selected NOESY correlations (**b**).

H-9, H-10 and H-18 to the remaining carbonyl carbon at 210.3 p.p.m. Therefore, the planar structure of compound **1** was determined.

The relative stereochemistry was examined by the phase-sensitive NOESY spectrum (Figure 2b). H-10 showed NOEs with H-12 at 0.78 p.p.m. and H-14 at 0.98 p.p.m., and these correlations suggested that the cyclohexane had a chair conformation and all three protons were assigned as axials. H-10 also had NOESY correlations with Me-11 and Me-15, allowing the assignments of their equatorial-orientations on the cyclohexane part, and a *cis*-configuration of the decalin moiety, which was also confirmed by NOEs between H-11 and Me-18, between Me-11 and H-9, and between Me-15 and H-18. These NOEs were also confirmed by β-orientation of Me-18 and α-orientation of the pyrrolizidinone moiety at C-9 position. Me-13 was assigned as an equatorial by the large coupling constants of $^{3}J_{\text{H-12ax/H-13}}$ and $^{3}J_{\text{H-13/H-14ax}}$, which suggested H-13 was an axial. It was also confirmed by the NOEs with both H-14axial and H-14equatorial. In the pyrrolizidinone moiety, an NOE between H-2a and H-7a was observed suggesting β-orientations of them, which also allowed the assignment of β-orientation of the hydroxyl group at C-7b. H-7 was assigned as α-orientation by the dihedral angle of H-7-C-7—C-7a-H-7a was approximately 90°, which were implied from the weak vicinal coupling between H-7 and H-7a. Based on all the above results, the structure of compound **1** was determined as shown in Figure 1 and designated as pyrrolizilactone.

The configuration between the decalin and pyrrolizidinone moieties could not be determined by NOESY spectrum due to free rotation at C-7 and C-9 positions, but NOEs between H-7 and H-9 and H-7 and H-18 were observed (Table 1). Therefore, there are four possible stereo-structures, which include two enantiomers and two diastereomers by the same relative stereochemistry.

Cytotoxic and antibacterial activities of compound **1** were evaluated *in vitro*. Compound **1** showed moderate cytotoxicities against human promyelocytic leukemia cell line HL-60 and human cervical cancer cell line HeLa with IC_{50} values of 1.1 and 3.1 μg ml^{-1}, respectively. In contrast, it did not show antibacterial activity against *Escherichia coli* up to 30 μg ml^{-1}. Two compounds, CJ-16264[12] and UCS1025A,[13] have been reported in the same class of metabolites (Figure 1), and show broad antibacterial activities against Gram-positive bacteria. It is worth evaluating such activities in future work. We have also observed morphological changes on cancer cell lines, and will report the findings elsewhere.

Compound **1** had a tricyclic skeleton composed of a pyrrolizidinone moiety fused with a γ-lactone, which was connected to a decalin moiety by a ketone. As mentioned above, only two compounds, UCS1025A and CJ-16264, have been reported in the same class of fungal metabolites, and the differences between them in terms of their planar structure lie in the substitution pattern of methyl groups on the decalin moiety. That of **1** was highly substituted with five methyl groups. UCS1025A, on the other hand, had only one methyl group. In terms of the stereochemistry, the pyrrolizidinone moiety had the same relative configuration as UCS1025A, with a *trans* configuration at H-7 and H-7a. The structure of CJ-16264 was shown to have a *cis*-configuration at H-7 and H-7a.[12] This could be a mistake, because Sugie *et al.*[12] determined the dihedral angle of H-7–C-7–C-7a–H-7a to be 84.9° through molecular mechanics calculations, which clearly suggests a *trans* configuration. The decalin unit of **1** had a *cis*-configuration, which is consistent with CJ-16264 but not with UCS1025A, which has a *trans* configuration.

ACKNOWLEDGEMENTS

We thank Drs T Nakamura and Y Hongo (RIKEN) for the HRESIMS measurements. We also thank Dr T Shimizu (RIKEN) for useful discussions on the structure. This work was supported in part by Technology of Japan, the Program for Promotion of Basic and Applied Researches for Innovations in Bio-oriented Industry, and a Health and Labor Sciences Research Grant.

1 Osada, H. An overview on the diversity of actinomycete metabolites. *Actinomycetol* **15,** 11–14 (2001).
2 Newman, D. J. & Cragg, G. M. Natural products as sources of new drugs over the 30 years from 1981 to 2010. *J. Nat. Prod.* **75,** 311–335 (2012).
3 Dobson, C. M. Chemical space and biology. *Nature* **432,** 824–828 (2004).
4 Osada, H. *Bioprobes* (ed. Osada, H.) 1–14 (Springer, Berlin, 2000).
5 Osada, H. *Chemical Biology Techniques and Applications* (ed. Osada, H.) 1–10 (Wiley, New Jersey, 2009).
6 Osada, H. & Nogawa, T. Systematic isolation of microbial metabolites for natural products depository (NPDepo). *Pure Appl. Chem.* **84,** 1407–1420 (2012).
7 Kato, N., Takahashi, S., Nogawa, T., Saito, T. & Osada, H. Construction of a microbial natural product library for chemical biology studies. *Curr. Opin. Chem. Biol.* **16,** 101–108 (2012).
8 Nogawa, T. *et al.* Verticilactam, a new macrolactam isolated from a microbial metabolite fraction library. *Org. Lett.* **12,** 4564–4567 (2010).
9 Nogawa, T. *et al.* Spirotoamides A and B, novel 6,6-spiroacetal polyketides isolated from a microbial metabolite fraction library. *J. Antibiot.* **65,** 123–128 (2012).
10 Panthee, S. *et al.* Furaquinocins I and J: novel polyketide isoprenoid hybrid compounds from *Streptomyces reveromyceticus* SN-593. *J. Antibiot.* **64,** 509–513 (2011).
11 Takahashi, S. *et al.* Biochemical characterization of a novel indole prenyltransferase from *Streptomyces* sp. SN-593. *J. Bacteriol* **192,** 2839–2851 (2010).
12 Sugie, Y. *et al.* New pyrrolizidinone antibiotics CJ-16,264 and CJ-16,367. *J. Antibiot.* **54,** 917–925 (2001).
13 Agatsuma, T. *et al.* UCS1025A and B, new antitumor antibiotics from the fungus Acremonium species. *Org. Lett* **4,** 4387–4390 (2002).

Supplementary Information accompanies the paper on The Journal of Antibiotics website (http://www.nature.com/ja)

ChemPubSoc Europe

DOI: 10.1002/cbic.201300499

Identification of a Molecular Target of a Novel Fungal Metabolite, Pyrrolizilactone, by Phenotypic Profiling Systems

Yushi Futamura,[a] Makoto Kawatani,[a] Makoto Muroi,[a, b] Harumi Aono,[a] Toshihiko Nogawa,[b] and Hiroyuki Osada*[a, b]

In the course of screening our microbial metabolite fraction library, we identified a novel pyrrolizidinone compound, pyrrolizilactone. In this study, we report the identification and characterization of a molecular target for pyrrolizilactone by using two phenotypic profiling systems. Cell morphology-based profiling analysis using an imaging cytometer (MorphoBase) classified pyrrolizilactone as a proteasome inhibitor. Consistently, proteome-based profiling analysis using 2D difference gel electrophoresis (DIGE; ChemProteoBase) also demonstrated that pyrrolizilactone is associated with proteasome inhibition. On the basis of these predictions, we determined that pyrrolizilactone is a novel type of proteasome inhibitor inhibiting the trypsin-like activity of the proteasome.

Introduction

In the development of anticancer drugs, natural products are highly valued and are considered as an irreplaceable source of novel drug candidates. Indeed, 74.9% of small-molecule anticancer drugs that have been approved worldwide since the instigation of chemotherapy at the beginning of 20th century were either derived from natural products or nature-inspired synthetic compounds.[1]

The discovery of structurally novel and biologically unique natural products has become more challenging with every year due, in part, to the limited number of screening lines. To overcome this, our group and other investigators have recently constructed and utilized a "microbial metabolite fraction library" as an effective way to promote a natural-product-based drug discovery program.[2] For the microbial metabolite fraction library, we made a systematic collection of chromatographically semipurified samples of microbial fermentation broths with various physicochemical properties (retention time, UV absorption profile, and MS spectral data of each detectable metabolite in the fractions), thereby forming an original microbial metabolite database, NPPlot.[3] By using a fraction library and NPPlot, we successfully uncovered hidden valuable metabolites based on their spectral data, despite their low quantities in fractions. Subsequent easy isolation and re-separation allowed us to identify novel and biologically potent compounds in many instances.[4]

Pyrrolizilactone is a novel fungal metabolite recently isolated from our fraction library.[5] This compound shows moderate cytotoxic activities against various cancer cell-lines and induces a unique morphological phenotype. The novel compound was isolated based on phenotype screening, and we subsequently sought to elucidate the mechanism of action. Two fundamentally distinct approaches exist for identifying molecular targets following phenotypic screening: direct and indirect.[6] The direct approach uses affinity chromatography, often with compound-immobilized beads. This approach can be exceptionally powerful and effective when the compound can easily be immobilized and the ligand compounds can be appropriately chemically modified. However, in the case of natural products, this is not often possible because of the low amounts available and their high structural complexity. In such instances, an indirect method can be more helpful in determining the mode of action of an agent. Accordingly, we reported two indirect target identification approaches—MorphoBase[7] and ChemProteoBase[8] profiling systems—based on specific changes in cellular morphology and on the intracellular proteome induced by chemical manipulations. Both techniques can identify possible molecular targets of compounds of interest by comparing their phenotypic responses to a reference dataset of the observed phenotypes of well-characterized anticancer drugs.

In this study, we report the identification and characterization of the molecular target of pyrrolizilactone with the aid of these two indirect phenotype profiling systems.

Results

Target prediction of pyrrolizilactone by MorphoBase profiling

We first investigated the growth inhibitory activity of pyrrolizilactone (Figure 1 A) against several cancer cell-lines: HeLa (human cervical carcinoma), HL-60 (human promyelocytic leu-

[a] Dr. Y. Futamura, Dr. M. Kawatani, Dr. M. Muroi, H. Aono, Prof. Dr. H. Osada
Antibiotics Laboratory, RIKEN
2-1 Hirosawa, Wako, Saitama 351-0198 (Japan)
E-mail: hisyo@riken.jp

[b] Dr. M. Muroi, Dr. T. Nogawa, Prof. Dr. H. Osada
Chemical Biology Research Group, RIKEN CSRS
2-1 Hirosawa, Wako, Saitama 351-0198 (Japan)

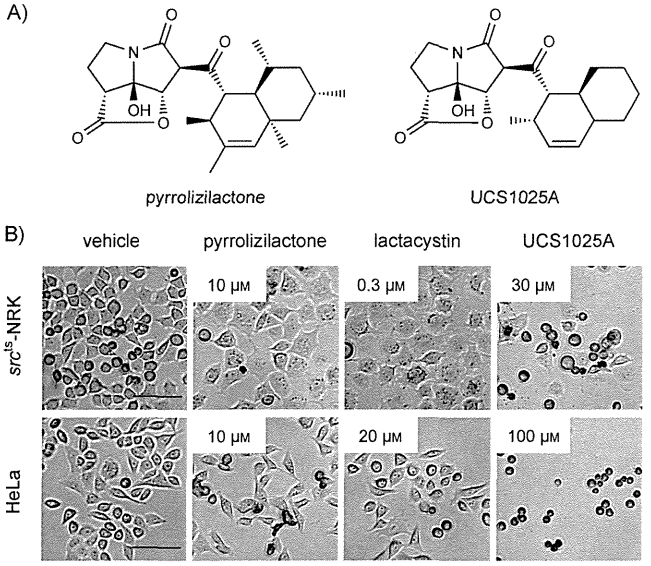

Figure 1. Structures and phenotype changes induced by pyrrolizilactone and UCS1025A. A) Chemical structure of pyrrolizilactone and UCS1025A. B) Representative images of morphological changes in *src*^{ts}-NRK and HeLa cells at 48 and 24 h, respectively, after treatment with pyrrolizilactone, lactacystin, or UCS1025A. Scale bars: 100 μm.

kemia), tsFT210 (mouse temperature-sensitive cdc2 mutant cell-line of the mammary carcinoma FM3A), and *src*^{ts}-NRK (rat kidney cells infected with ts25, a T-class mutant of Rous sarcoma virus Prague strain). Pyrrolizilactone displayed moderate cytotoxic effects against these cell-lines with sub-micromolar IC_{50} values (Table 1). Additionally, the cells exhibited unique morphological changes, similar to those induced by proteasome inhibitors, such as lactacystin (Figure 1 B).

MorphoBase profiling was performed to elucidate the details of the mechanism of action of pyrrolizilactone. Following treatment, the nuclei were stained with Hoechst33342 and the resulting morphological changes in *src*^{ts}-NRK and HeLa cells were distinguished and quantified by an IN Cell Analyzer (GE Healthcare). The obtained multiple phenotypic parameters were compared against the reference dataset (a compilation of morphological features induced by 211 compounds) and subjected to statistical analysis: principal component analysis (PCA), probability scores, and ranking of the top 15 nearest neighbors. Regarding the projection of PCA scores, the phenotypic responses of pyrrolizilactone were visible near the cloud of proteasome inhibitors in the PC1–PC2 scatter plots (Figure 2). Based on the similarity analysis, pyrrolizilactone was also predicted to be associated with the inhibition of the proteasome ($Score_{proteasome} = 1.71$; Table 2). Proteasome inhibitors were typical listed among most of its 15 closest neighbors (Table 2), thus indicating that the molecular target of pyrrolizilactone is putatively a proteasome.

Table 1. IC_{50} values [μM] of pyrrolizilactone and UCS1025A against growth of various cancer cell-lines.

Cell-line	pyrrolizilactone	UCS1025A	Cell-line	pyrrolizilactone	UCS1025A
HeLa	9.5	57.9	tsFT210	15.8	63.8
HL-60	2.5	17.0	*src*^{ts}-NRK	11.7	18.8

A human telomerase inhibitor, UCS1025A (Figure 1 A),[9,10] was one of the few compounds that are structurally related to pyrrolizilactone. Therefore, the effects of UCS1025A on cell morphological changes in *src*^{ts}-NRK and HeLa cells were examined. The observed IC_{50} values and phenotypes were distinct from those of pyrrolizilactone (Table 1 and Figure 1 B), thereby generating a marked difference between pyrrolizilactone and UCS1025A in the MorphoBase profiling results (Table 3).

Target prediction of pyrrolizilactone by ChemProteoBase profiling

To verify these predictions, pyrrolizilactone was subjected to ChemProteoBase profiling. The proteomic variation of 296 spots that matched on all gel images was quantified, followed by the performance of hierarchical cluster analysis as previous-

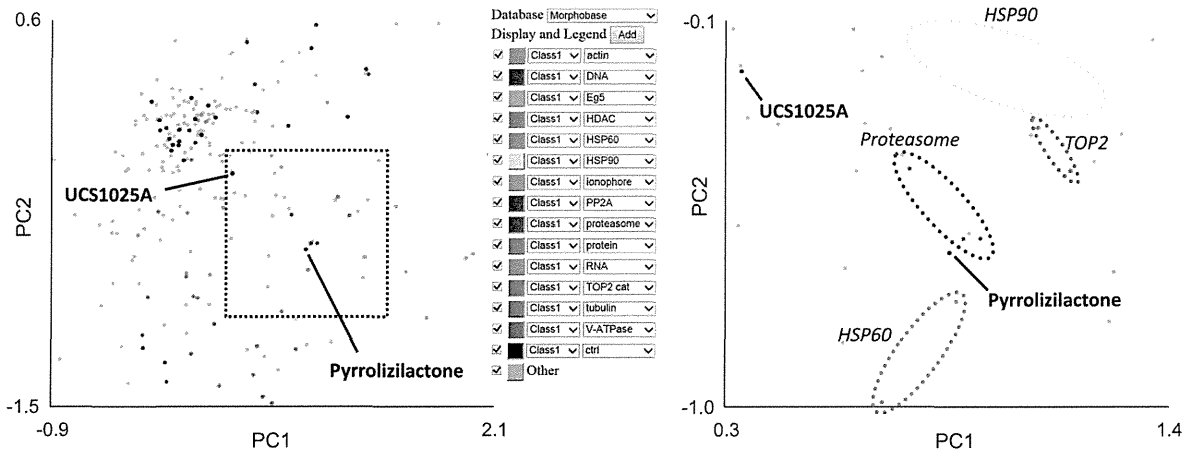

Figure 2. Target prediction of pyrrolizilactone by MorphoBase Profiling. *src*^{ts}-NRK and HeLa cells were treated with pyrrolizilactone (20 and 10 μM, respectively) or UCS1025A (20 and 25 μM, respectively), and the resulting phenotype multiparameters were subjected to MorphoBase analysis. PCA scores of pyrrolizilactone and UCS1025A were projected onto PC1–PC2 2D scatter plots (PC = principal component).

Table 2. Similarity scores for pyrrolizilactone determined by MorphoBase profiling.

Probability scores[a]			Similarity ranking[b]					
Rank	Class	Score	Rank	Sample	Class	Target	MOA[c]	Distance
1	proteasome	1.71	1	ETB	HSP60	HSP60	heat shock protein	0.530
2	DNA	1.78	2	MG132	proteasome	26S proteasome	proteasome	0.630
3	ionophore	2.14	3	brefeldin A		ARFGEF	vesicle trafficking	0.710
4	HSP60	2.21	4	GN26361	HSP60	HSP60	heat shock protein	0.710
5	Eg5	2.49	5	purvalanol		CDK1/2	cyclin dependent kinase	0.760
6	actin	2.82	6	lactacystin	proteasome	20S proteasome	proteasome	0.780
7	V-ATPase	3.17	7	ALLN	proteasome	proteasome, calpain, cathepsin	proteasome	0.810
8	RNA	3.33	8	nigericin	ionophore	K^+	vesicle trafficking	0.860
9	HSP90	3.54	9	terpendole E	Eg5	Eg5	microtubule dynamics	0.870
10	tubulin	4.22	10	indirubin-3′-monoxime		GSK3β	GSK3β	0.880
11	control	4.35	11	MDM2 inhibitor		MDM2	MDM2	0.890
12	HDAC	5.52	12	manumycin A		FTase/GGTase	second messenger	0.890
13	protein	5.78	13	rotenone		complex I, tubulin	mitochondria respiration	0.900
14	PP2A	6.36	14	nutlin-3		MDM2	MDM2	0.900
15	TOP2 cat	6.45	15	reversine		MPS1	mitotic kinase	0.910

[a] Probability scores show the ranking of the likely mode of action for pyrrolizilactone among 14 well-validated target classes in the training set. [b] The similarity ranks of the 15 closest neighbors for pyrrolizilactone were determined by Euclidean distance between pyrrolizilactone and reference compounds. [c] MOA = mode of action.

Table 3. Similarity scores for UCS1025A determined by MorphoBase profiling.

Probability scores[a]			Similarity ranking[b]					
Rank	Class	Score	Rank	Sample	Class	Target	MOA[c]	Distance
1	DNA	1.34	1	AZT		reverse transcriptase	reverse transcriptase	0.620
2	ionophore	1.89	2	dephostatin		PTP	phosphatase	0.690
3	proteasome	2.27	3	α-amanitin	RNA	RNA polymerase	RNA synthesis	0.690
4	HSP90	2.49	4	MEK inhibitor I		MEK	MAPK pathway	0.700
5	RNA	2.56	5	nalidixic acid		reverse transcriptase	reverse transcriptase	0.710
6	Eg5	2.69	6	akt inhibitor XI		AKT	AKT	0.710
7	actin	3.32	7	benzylguanine		DNMT	epigenetics	0.720
8	control	3.32	8	fumonisin B1		sphingosine N-acyltransferase	sphingosine N-acyltransferase	0.720
9	V-ATPase	3.57	9	nutlin-3		MDM2	MDM2	0.730
10	HSP60	3.98	10	MDM2 inhibitor		MDM2	MDM2	0.740
11	tubulin	4.02	11	nordihydroguaiaretic acid		lipoxygenase	lipoxygenase	0.750
12	HDAC	4.72	12	ABT-702		adenosine kinase	anti-inflammatory	0.760
13	protein	6.15	13	control10	control			0.760
14	PP2A	6.24	14	mitomycin C	DNA	DNA	DNA synthesis	0.770
15	TOP2 cat	6.35	15	BESpm		SSAT	SSAT	0.770

[a] Probability scores show the ranking of the likely mode of action for UCS1025A among 14 well-validated target classes in the training set. [b] The similarity ranks of the 15 closest neighbors for UCS1025A were determined by Euclidean distance between UCS1025A and reference compounds. [c] MOA = mode of action.

ly described[8] and calculation of cosine similarities of compounds in the database against pyrrolizilactone. As expected from MorphoBase profiling, hierarchical cluster analysis with 42 standard compounds revealed that pyrrolizilactone was in the cluster of proteasome and HSP90 inhibitors (Figure 3). Pyrrolizilactone shared predominant phenotypic features with MG-132 and proteasome inhibitor II among the 110 compounds contained in the ChemProteoBase; lactacystin also scored highly in the similarity ranking (Table 4). Among the 296 spots, proteins markedly increased or decreased in HeLa cells treated with pyrrolizilactone are listed in Table 5. HSP70 and HSP27 have been reported to be upregulated in cells treated with proteasome or HSP90 inhibitors.[11] In pyrrolizilactone-treated cells, the expression levels of spots 934, 949, and 1975 (identified as heat shock 70 kDa protein 1A/1B) were significantly increased, as for cells treated with proteasome or HSP90 inhibitors. Spots 1754 and 1757 (identified as HSP27) were also increased in cells treated with both proteasome and HSP90 inhibitors. However, in proteasome-inhibitor-treated cells, the spots were observed to increase at a greater rate than those in HSP90-inhibitor-treated cells. A similar trend was observed for HSP27 spot expression in pyrrolizilactone-treated cells. These data suggested that the proteasome is the most promising target for pyrrolizilactone action.

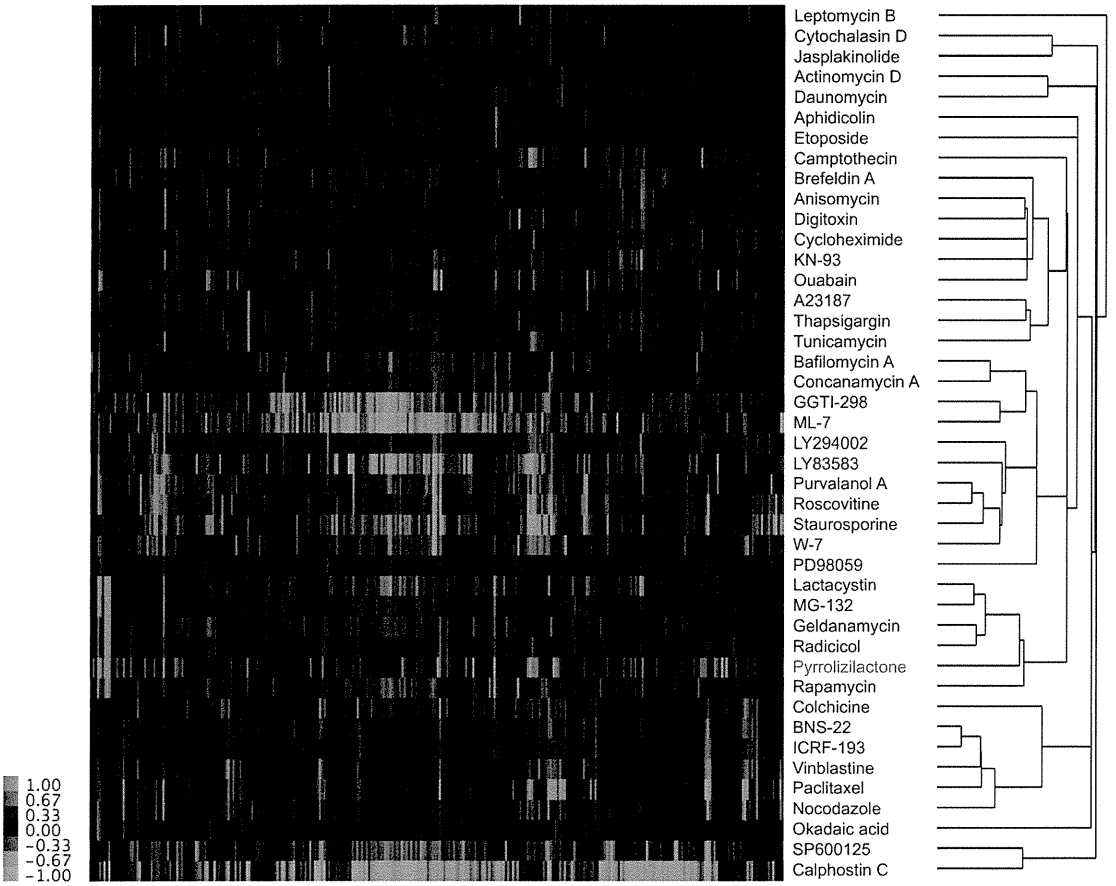

Figure 3. Analysis by ChemProteoBase profiling. HeLa cells were treated with 20 μM pyrrolizilactone for 18 h. Proteomic analysis of cell lysates was performed by the 2-D DIGE system. Quantitative data of the common 296 spots (*x*-axis) derived from pyrrolizilactone and those of 42 well-characterized compounds were analyzed by hierarchical clustering. In the heat map, log-fold (natural base) of the normalized volume is shown on the colored scale.

Table 4. Similarity scores for pyrrolizilactone determined by ChemProteoBase profiling.[a]

Ranking	Similarity	Compound	Target	Similarity	
1	0.72	MG-132	proteasome	>0.8	
2	0.72	proteasome inhibitor II	proteasome	0.7 to 0.8	**
3	0.68	ethacrynic acid	GST inhibitor	0.6 to 0.7	***
4	0.67	radicicol	HSP90	0.5 to 0.6	***
5	0.63	lactacystin	proteasome	0.4 to 0.5	**********
6	0.58	MEK inhibitior I	MEK	0.3 to 0.4	**********
7	0.58	rapamycin	TOR	0.2 to 0.3	**********
8	0.54	geldanamycin	HSP90	0.1 to 0.2	**********
9	0.50	aclacinomycin A	topo I, topo II, proteasome	0.0 to 0.1	********
10	0.50	novobiocin	HSP90, GFP	−0.1 to−0.0	*
				−0.2 to −0.1	

[a] Cosine similarity between pyrrolizilactone and each compound in ChemProteoBase was calculated, and a top-ten list of compounds similar to pyrrolizilactone in ranking is displayed in the left-hand table. Based on the similarity, a histogram of the compounds in ChemProteoBase is displayed in the right-hand figure.

Pyrrolizilactone inhibits proteasome activities

The results of our phenotypic profiling studies prompted speculation that pyrrolizilactone inhibits proteasome activity. To test this hypothesis, human 20S proteasome was incubated with the agent, and the chymotrypsin-like, trypsin-like, and caspase-like activities of the proteasome were measured by using specific fluorogenic peptides. Pyrrolizilactone markedly inhibited proteasome activities in a dose-dependent manner, especially for trypsin-like activity (IC_{50} (trypsin-like) = 1.6 μM; IC_{50} (chymotrypsin-like) = 29 μM; IC_{50} (caspase-like) = 84 μM), whereas UCS1025A minimally inhibited proteasome activity (Figure 4A and Table 6). Interestingly, MG-132 (as well as bortezomib)[12] primarily inhibited chymotrypsin-like activity in vitro (Figure 4A and Table 6), thus suggesting that pyrrolizilactone